PERIÓDICO TCHÊ QUÍMICA
ARTIGO ORIGINAL

PULVERIZAÇÃO POR MAGNETRON DE FILMES FINOS NANOCRISTALINOS DE TiN E PROPRIEDADES DE CORROSÃO

MAGNETRON SPUTTERED NANOCRYSTALLINE TiN THIN FILMS AND CORROSION PROPERTIES

خصائص التأكل للأغشية الرقيقة النانوية TiNالمحضرة بطريقة الترذيذ الماكتنروني للتيارات المستمرة

HAMIL, Muslim Idan[1*], KHALAF, Mohammed K[2], AL-SHAKBAN, Mundher[3]

[1,3] Department of Physics, Faculty of Science, University of Misan, Maysan, Iraq.

[2] Center of Applied Physics, Directorate of Materials Research, Ministry of Science and Technology, Baghdad, Iraq.

** Corresponding author*
e-mail: muslim.iddan@uomisan.edu.iq

Received 26 March 2020; received in revised form 01 May 2020; accepted 16 May 2020

RESUMO

Neste relatório, filmes finos nanocristalinos de TiN foram depositados em substratos de vidro e Ti-6Al-4V utilizando o processo de pulverização por magnetron DC. Os filmes de TiN foram pulverizados usando um alvo de Ti puro (99,9%) com 40W de potência em atmosfera de mistura de gás Ar/N_2. A estrutura dos filmes de TiN foi caracterizada por difração de raios-X, já que os filmes preparados exibiam uma orientação preferida (200), enquanto o filme recozido a 500 °C mostra os (111), (200) e (311). Filmes de TiN policristalinos, cúbicos e orientados a (111) foram produzidos com temperatura de recozimento de 500 °C. O efeito da temperatura depositada nas morfologias microestruturais dos filmes finos foi estudado por Microscópio Eletrônico de Varredura por Emissão de Campo (FESEM). O tamanho das partículas dos filmes de TiN pulverizados variou de 50 a 70 nm e foi fortemente influenciada pelas temperaturas de recozimento, a morfologia dos filmes depositados antes e após o recozimento apresenta uma aglomeração característica de partículas. A análise de polarização potenciodinâmica dos filmes de TiN confirma a relação inversa entre resistência de polarização e corrente de corrosão. Também foram obtidas as medidas de biocorrosão para filmes de TiN depositados no substrato Ti-6Al-4V em solução de NaCl a 3,5%. Foi observada uma clara melhoria na resistência à corrosão, e em oposição as não tratadas, especialmente para amostras de TiN/Ti-6Al-4V com recozimento térmico (500 °C). A taxa de corrosão foi de 0,1458 mm/ano para a amostra não revestida, enquanto que nas amostras de TiN/Ti-6Al-4V após o recozimento foi de $2{,}668 \cdot 10^{-4}$ mm/ano. O potencial médio de corrosão calculado foi 0,117 V. Os resultados confirmaram que as ligas revestidas com tratamento térmico a 500 °C exibiram um melhor comportamento eletroquímico em comparação com as ligas não revestidas e não tratadas termicamente, possivelmente devido ao melhor grau de coesão dos revestimentos.

Palavras-chave: *Técnica PVD, filmes finos, nitreto de titânio, liga Ti-6Al-4V, biocorrosão.*

ABSTRACT

In this report, TiN nanocrystalline thin films were deposited on glass and Ti-6Al-4V substrates using a DC-magnetron sputtering technique. The TiN films were sputtered using a pure Ti target (99.9%) with 40W of power in Ar/N_2 gas mixture atmosphere. The structure of the TiN films was characterized by X-Ray diffraction, as prepared films exhibited a (200) preferred orientation, while film annealed at 500 °C shows the (111), (200) and (311). Polycrystalline, cubic, (111)-orientated TiN films were produced by annealing temperature of 500 °C. The effect of deposited temperature on the microstructural morphologies of the thin films was studied by Field Emission Scanning Electron Microscope (FESEM). The particle size of the sputtered TiN films ranged from 50 to 70 nm and was strongly influenced by annealing temperatures, the morphology of the films deposited before and after annealing has a characteristic agglomeration of particles. Potentiodynamic polarization analysis of the TiN films confirms the inverse relationship between polarization resistance and corrosion current. The biocorrosion measurements for TiN films deposited on the Ti-6Al-4V substrate in 3.5% NaCl solution have also been obtained. Clear improvement in the corrosion resistance was observed rather than for untreated, especially for thermally annealed (500 °C) TiN/Ti-6Al-4V samples. The corrosion rate was 0.1458 mm/y for the uncoated sample, while $2.685 \cdot 10^{-4}$ mm/y for TiN/Ti-6Al-4V in samples after annealing. The average corrosion

Downloaded from www.periodico.tchequimica.com

DOI: 10.52571/PTQ.v17.n35.2020.15_HAMIL_pgs_164_173.pdf

potential calculated was - 0.117 V. The results confirmed that coated alloys with 500 °C thermally treated exhibited a better electrochemical behavior compare with uncoated and non-thermally treated alloys possibly due to the better cohesion degree of the coatings.

Keywords: *PVD technique, thin films, titanium nitride, Ti-6Al-4V alloy, biocorrosion.*

الملخص

في هذا البحث، تم اجراء هذه الدراسة من اجل زيادة مقاومة التأكل البيولوجي للأغشية الرقيقة النانوية TiN المرسبة بإحدى طرائق التبخير الفيزيائية (Physical Vapor Deposition). تم ترسيب الاغشية الرقيقة النانوية TiNعلى ركائز الزجاج وسبيكةTi-6Al- 4V باستخدام تقنية الترذيذ الماكنتروني للتيارات المستمرة. حيث تم ترذيذ الاغشية الرقيقة باستخدام هدف من التيتانيوم النقي (Ti) بقدرة 40 W تحت خليط من غاز الأركون والنيتروجين Ar/N_2 . شخص التركيب البلوري للأغشية الرقيقة TiNباستخدام تقنية حيود الاشعة السينية X-Ray. حيث أظهرت الاغشية الرقيقة المطلية على الزجاج اتجاها (200)، بينما بعد التلدين وعند درجة حرارة 500 درجة مئوية أظهرت مزيج من الاتجاهات (111)، (200) و (310). نستنتج من ذلك ان الغشاء الرقيق TiN ذات اتجاه (111)، مكعبي وPolycrystalline. بعد ذلك، تم دراسة تأثير الحرارة على التركيب النانوي للغشاء الرقيق المشخص باستخدام المجهر الالكتروني الماسح (FE-SEM)، وبفعل المعالجة الحرارية، ازداد الحجم الحبيبي للأغشية الرقيقة من 50 الى 70 نانومتر مع زيادة تكتل الحبيبات النانوية للغشاء الرقيق. لقياسات التأكل البيولوجي، تم غمر السبيكة Ti-6Al-4V المطلية بالغشاء الرقيق TiN في محلول كلوريد الصوديوم وبنسبة (3.5% NaCl)، اذ تم حساب التاكل البيولوجي لهذا السبائك المطلية وغير المطلية من خلال Potentiodynamic Polarization, لوحظ ان مقاومة التأكل للغشاء الرقيق الملدن ازدادت بشكل واضح، بالإضافة الى ان معدل التأكل للسبيكة النقية (غير المطلية) mm/y0.1458 mm/y0.1458 ، بينما معدل التأكل للسبيكة المطلية والملدنة انخفض الى 2.685×10^{-4} mm/y بالمقارنة مع السبيكة النقية. أظهرت النتائج أن المعالجة الحرارية حسنت من صفات السبيكة المطلية والمعالجة حراريا عند درجة حرارة 500 درجة مئوية وايضا أظهرت هذه السبائك سلوكًا كهروكيميائيًا أفضل بالمقارنة مع السبائك غير المطلية وغير الملدنة ربما بسبب درجة التماسك الأفضل للطلاء.

الكلمات المفتاحية: تقنية الترسيب التبخير الفيزيائية, الاغشية الرقيقة, نيتريد التيتانيوم, سبيكة Ti-6Al-4V, التأكل البيولوجي

1. INTRODUCTION:

Titanium nitride has shown its potential application in various industries including an anti-corrosive coating or a hard coating on cutting tools because of its important properties such as corrosion resistance and high hardness (Borah, Pal, Bailung, and Chutia, 2008; Fenker, Balzer, Kappl, and Banakh, 2005). TiN thin films have been prepared using several methods such as electrodeposition (Ma, Jiang, and Xia, 2017), dynamic mixing (Takano, Isobe, Sasaki, and Baba, 1989), hollow cathode discharge ion plating(Chou, Yu, and Huang, 2001), and pulsed laser deposition (Xu, Du, Sugioka, Toyoda, and Jyumonji, 1998). However, DC-magnetron sputtering was mostly used to deposit TiN thin films, and this method presents a high ionization rate (> 40 %) which make it a good technique to obtain dense coatings (Kouznetsov, Macak, Schneider, Helmersson, and Petrov, 1999; Manouchehri, AlShiaa, Mehrparparvar, Hamil, and Moradian, 2016; Paulitsch, Mayrhofer, Münz, and Schenkel, 2008; Paulitsch, Schenkel, Zufraß, Mayrhofer, and Münz, 2010), as well as good mechanical properties, increase the adhesion between the film and the ceramics and/or metals substrates (Schönjahn *et al*., 2000). The deposition of TiN using magnetron sputtering has significant specific advantages such as low levels of impurities and easy control of the deposition rate. This method enables the production of thin films in various morphology and crystallographic structures (Kelly and Arnell, 2000; Khalaf, Hassan, Khudiar, and Salman, 2020).

The use of Ti and TiN films as protective coatings is rapidly growing so that it is important to know their corrosion properties. Also, Ti compounds and its alloys such as Ti-6Al-4V and TiN, in particular, are being increasingly used as biomaterials (Manso-Silvan, Martínez-Duart, Ogueta, García-Ruiz, and Pérez-Rigueiro, 2002), they also have excellent properties, e.g., biocompatibility, corrosion resistance, low density, mechanical strength, and relatively low cost. These properties make titanium and its alloys a potential dental implant material. Among these features, the corrosion resistance is of great importance, not only because it determines the device's service life, but also because of the harmfulness of the corrosion processes taking place in the living organismo (Veiga, Davim, and Loureiro, 2012).

This paper reports data for TiN thin films grown on glass and Ti-6Al-4V substrates by using DC magnetron-sputtering deposition. The corrosion behavior was investigated by measuring the polarization curve (Tafel). We focus on the annealing temperature in controlling the structural and corrosion properties of the TiN films produced.

2. MATERIALS AND METHODS:

2.1. Experimental

TiN thin films were deposited on glass,

Downloaded from www.periodico.tchequimica.com

and Ti6Al4V substrates by D.C were sputtering. The glass substrates were cleaned ultrasonically by ethanol and deionized water for 15 min before sputtering and then loaded to the substrate holder of the sputtering machine. Corning # 7059 glasses (30 × 40×1.2 mm^3) were used, while the Ti-6Al-4V samples were cut to 20 mm × 20 mm diameter then grinded by 500 microns SiC grinding paper. The substrates were cleaned by using ultrasonic twice in ethanol 96% (Sigma Aldrich, England), then by distilled water for 15 min and allowed to dry in discaiter at room temperature for 24 h (Hamil, Siyah, and Khalaf, 2020). The sputtering target was a pure Ti disc (99.99%, 2 inches, and diameter 5 mm thick). The base pressure was $1{\cdot}10^{-5}$ Torr, and the sputtering was carried out in Ar:N_2 (90:10) atmosphere. Before starting the deposition, the target was pre-sputtering for 15 min with a shutter located between the target and substrate. During all depositions, the target to substrate distance and sputtering power were adjusted at 60 mm and 40 W, respectively. The pressure of the sputtering chamber was pumped down to $5{\cdot}10^{-3}$ Torr before deposition. Then nitrogen gas was introduced into the chamber, and the required pressure was set. After that, argon gas was introduced until the preset pressure was reached.

When the preset total pressure was reached, the nitrogen was shut off, and the target was preset in an argon atmosphere for around 10 min to avoid the target's surface oxide layer. After presputtering, the nitrogen gas was again introduced into the chamber with a flow rate ratio of Ar(90)/N_2(10), and the sputtering process starts. The sputtering conditions are listed in Table 1.

The structural properties of TiN films were obtained by the X-ray diffraction (Philips Geiger using CuKα ($\lambda = 1.54$ Å). The FE-SEM (TESCAN MIRA3) was used to observe the morphology of the films. The corrosion process was determined using ASTM G1-03/ASTM G102, and the corrosion behavior was investigated by measuring the polarization curve (Tafel).

3. RESULTS AND DISCUSSION:

3.1 X-Ray diffraction

Figuere 2 shows X-ray diffraction patterns of the samples before and after heat treatment at 500 °C for 2 h. The low intensity of the X-ray diffraction peaks, as well as its large widths, clearly indicates that the deposited films are not fully crystalline and that a large fraction of the films are still amorphous and are in agreement with previous studies (Vasu, Krishna, and Padmanabhan, 2011). As-deposited Titanium nitride films deposited before thermal annealing shows a single crystalline peak corresponding to a plane (200) at 2θ =36.86° for comparison (JCPDS file number 77-1893) (Vasu *et al.*, 2011). The Bragg angle of the plane (200) had shifted to another angle. Close examination of the XRD pattern of the thermally annealed films deposited at 500°C with deposition time 2 h revealed that the tetragonal TiN phase had appeared more clearly with planes (111) and (311) (Chawla, Jayaganthan, and Chandra, 2008; Fenker *et al.*, 2005). At 500 °C thermally annealed thin films, the intensity of the Bragg reflections had increased in comparison with the as deposited thin films, at higher annealing temperatures, thermal energy enhances the mobility of the active sites, and this leads to grain growth (Kavitha, Kannan, Reddy, and Rajashabala, 2016), which is evidence for improved crystallinity.

The XRD pattern of the deposited film shows a weak peak at 37°, which can be related to the (111) crystallographic orientations of TiN with a face-centered cubic (FCC) structure (JCPDS card number 02-1159) (Kavitha *et al.*, 2016). It is known that the FCC structure of TiN may form when nitrogen atoms occupy all the octahedral sites of titanium with hexagonal close-packed (HCP) or body-centered cubic (BCC) structures. This transformation in titanium structure from HCP and BCC to FCC occurs due to the accommodation of nitrogen atoms with a small size in the interstitial sites of Ti with the larger size. The absence of a titanium peak in the XRD pattern demonstrates the absence of Ti atoms in the structure of the films and completes the nitride formation process. The competition between the surface energy, the strain energy, and the stopping energy of different lattice planes of a film affect the preferred orientation and lowest total energy of the film (Pelleg, Zevin, Lungo, and Croitoru, 1991; Zhao *et al.*, 1997). In the case of TiN film, the direction of the lowest energy is (111) direction. Annealing, the film did not influence the preferred orientation but increased the intensity of the peak. By increasing the annealing temperatures to 500 °C, TiN (111), peak intensity is increased. Thermal energy produced by annealing leads to the enhancement of mobility of active sites. The increase of mobility can be attributed to grain growth and the reduction of defects during the annealing treatment (Wang *et al.*, 2013).

Downloaded from www.periodico.tchequimica.com

3.2 Surface morphology of the TiN layers

Typical FESEM images of TiN films deposited on glass substrates under different deposition currents, before and after annealing at 400 and 500 °C, are shown in figure 3 (a – f). The amorphous particles and nonuniform clumps were observed before heat treatment. The agglomeration of the particles resulted in the formation of clusters. The FESEM micrograph of as-deposited TiN revealed that the average particle size of TiN is in the range of (25 nm). It is found that the TiN crystallite size has been increased after annealing, where the average particle size of TiN coated at 400, and 500 ^{o}C increased to 50 nm to 70 nm, respectively. The increase in annealing temperature (i.e., The crystallinity of the film increases), provides extra energy to the adatoms and results in increasing order of the microstructure and particle size. However, the excessive supply of annealing temperature may cause a degradation of the preferred orientation, and the film will suffer from the bombardment of highly energized particles, resulting in internal defects of the film (Chen, McEwen, Zaveri, Karpagavalli, and Zhou, 2012).

3.3 Corrosion measurements

Various electrochemical techniques have been applied to study the behavior of corrosion, for example, potentiodynamic polarization (Tafel analysis). Tafel analysis is a well-established electrochemical technique, and the current is recorded when the open-circuit potential is imposed on a metal sample. The corrosion rate calculated from combined Equation 1 and 2 (Chen *et al.*, 2012; Hamil *et al.*, 2020), polarization resistance (R_p) has an inverse relationship with corrosion current.

$$I_{corr} = \frac{\beta_a x \beta_c}{2.3\, R_P\ (\beta_a+\beta_c)} \qquad \text{(Eq. 1)}$$

Where, β_a = anodic Tafel slope, β_c=cathodic Tafel slope.

$$\text{Corrosion Rate (C.R)} = \frac{I_{corr} \times K \times EW}{d \times A} \qquad \text{(Eq. 2)}$$

K= constant that define the units of the corrosion rate = 3.272·10^{-3} mm/(μA year), EW= equivalent weight (g/equivalent) = 11.768 g/eq., d = density (g/cm^3) = 4.420 g/cm^3, A = sample area (cm^2) = 0.151 cm^2.

The polarization curve (Tafel) diagram for TiN coated on Ti6Al4V alloy were presented in figure (4). When the Ti6Al4V alloy was immersed in simulated biological 3.5% NaCl solution (Bodunrin, Chown, van der Merwe, and Alaneme, 2018; Bodunrin, Chown, van der Merwe, and Alaneme, 2019; Dai, Zhang, Zhang, Chen, and Wu, 2016), the average corrosion potential is (-0.117) V. The corrosion potential shifted to the cathode side for samples coated with TiN before, and after annealing, the potential values were -0.0547 and -0.048 V, respectively. Moreover, the corrosion current I_{corr} was obtained from the polarization curves by extrapolation of the anodic and the cathodic branches of the polarization curve to the corrosion potential. The corrosion current of TiN films before and after annealing were 4.6323·10^{-8} and 4.6541·10^{-9} A/cm^2, respectively. Also, the corrosion rate of coated samples was lower compared with Ti-6Al-4V alloy, and this was expected because the reduction in corrosion rate means the reduction in weight loss from sample material. The weight loss (W) was calculated from Equation 3 (Hamil *et al.*, 2020), Table (2).

$$W = Corr.Rate\ \frac{mm}{y} \times \rho\ \times 3.17 \times 10^{-9} \qquad \text{(Eq. 3)}$$

Also, open-circuit potential (OCP) is the other typical technique to study the corrosion. Figure (5) shows the variation of OCP with immersion time for TiN coated Ti-6Al-4V alloy in 3.5 NaCl% solution at 25 ^{o}C. The initial OCP for uncoated Ti-6Al-4V was - 0.772 V, the potential gradually increased to be - 0.512 and 0.067 V for the samples TiN coated before and after thermal annealing.

In general, the coated samples show a positive shift in corrosion potential value and decreasing in both corrosion current and corrosion rate values in comparison with the bare substrate. Moreover, a positive shift in corrosion potential value and decreasing in both corrosion current and corrosion rate values with thermal annealing are observed. These results can be ascribed to the formation of a passive layer.

4. CONCLUSIONS:

TiN films were prepared by DC-magnetron sputtering technique, film annealed at 500 ^{o}C exhibited cubic phase TiN. It has been observed that the particle sizes and corrosion properties were strongly influenced by temperature

Downloaded from www.periodico.tchequimica.com

annealing, where the average particle size increased to 50 and 70 nm for the films heated at 400 and 500 °C. The corrosion rate of TiN film deposited on Ti-6Al-4V substrate decreased, where it was 0.1458 mm/year for uncoated sample while being $2.685 \cdot 10^{-4}$ mm/year TiN for the sample annealed at 500 °C, this sample also presents the polarization resistance (R_P) of 3247 KΩ/cm^2, while it was 1.719 KΩ/cm^2 for the uncoated sample.

6. REFERENCES:

1. Bodunrin, M. O., Chown, L. H., van der Merwe, J. W., and Alaneme, K. K. (2018). Corrosion behavior of Ti-Al-xV-yFe experimental alloys in 3.5 wt% NaCl and 3.5 M H_2SO_4. *Materials* and *Corrosion, 69*(6), 770-780.
2. Bodunrin, M. O., Chown, L. H., van der Merwe, J. W., and Alaneme, K. K. (2019). Corrosion behaviour of low-cost Ti4.5 Al–x V–y Fe alloys in sodium chloride and sulphuric acid solutions. *Corrosion Engineering, Science* and *Technology, 54*(8), 637-648.
3. Borah, S. M., Pal, A. R., Bailung, H., and Chutia, J. (2008). Optimization of plasma parameters for high rate deposition of titanium nitride films as protective coating on bell-metal by reactive sputtering in cylindrical magnetron device. *Applied Surface Science, 254*(18), 5760-5765.
4. Chawla, V., Jayaganthan, R., and Chandra, R. (2008). Structural characterizations of magnetron sputtered nanocrystalline TiN thin films. *Materials characterization, 59*(8), 1015-1020.
5. Chen, Q., McEwen, G. D., Zaveri, N., Karpagavalli, R., and Zhou, A. (2012). Corrosion resistance of Ti–6Al–4V with nanostructured TiO_2 coatings *Emerging Nanotechnologies in Dentistry* (pp. 165-179): Elsevier.
6. Chou, W.-J., Yu, G.-P., and Huang, J.-H. (2001). Deposition of TiN thin films on Si (100) by HCD ion plating. *Surface* and *Coatings Technology, 140*(3), 206-214.
7. Dai, N., Zhang, L.-C., Zhang, J., Chen, Q., and Wu, M. (2016). Corrosion behavior of selective laser melted Ti-6Al-4 V alloy in NaCl solution. *Corrosion Science, 102*, 484-489.
8. Fenker, M., Balzer, M., Kappl, H., and Banakh, O. (2005). Some properties of (Ti, Mg) N thin films deposited by reactive dc magnetron sputtering. *Surface* and *Coatings Technology, 200*(1-4), 227-231.
9. Hamil, M. I., Siyah, M. A., and Khalaf, M. K. (2020). Electrophoretic deposition of Thin film TiO_2 on Ti_6AL_4V alloy surface for biomedical applications. *Egyptian Journal of Chemistry*.
10. Kavitha, A., Kannan, R., Reddy, P. S., and Rajashabala, S. (2016). The effect of annealing on the structural, optical and electrical properties of Titanium Nitride (TiN) thin films prepared by DC magnetron sputtering with supported discharge. *Journal of Materials Science: Materials in Electronics, 27*(10), 10427-10434.
11. Kelly, P. J., and Arnell, R. D. (2000). Magnetron sputtering: a review of recent developments and applications. *Vacuum, 56*(3), 159-172.
12. Khalaf, M. K., Hassan, N., Khudiar, A., and Salman, I. (2020). Photoconductivities of Nanocrystalline Vanadium Pentoxide Thin Film Grown by Plasma RF Magnetron Sputtering at Different Conditions of Deposition. *Physics of the Solid State, 62*(1), 74-82.
13. Kouznetsov, V., Macak, K., Schneider, J. M., Helmersson, U., and Petrov, I. (1999). A novel pulsed magnetron sputter technique utilizing very high target power densities. *Surface* and *Coatings Technology, 122*(2-3), 290-293.
14. Ma, C., Jiang, M., and Xia, F. (2017). Preparation and characterization of Ni–TiN thin films electrodeposited with nickel baths of different TiN nanoparticle concentration. *Surface Review* and *Letters, 24*(05), 1750063.
15. Manouchehri, I., AlShiaa, S. A. O., Mehrparparvar, D., Hamil, M. I., and Moradian, R. (2016). Optical properties of zinc doped NiO thin films deposited by RF magnetron sputtering. *Optik, 127*(20), 9400-9406.
16. Manso-Silvan, M., Martínez-Duart, J., Ogueta, S., García-Ruiz, P., and Pérez-Rigueiro, J. (2002). Development of human mesenchymal stem cells on DC sputtered titanium nitride thin films.

Downloaded from www.periodico.tchequimica.com

Journal of Materials Science: Materials in Medicine, 13(3), 289-293.

17. Paulitsch, J., Mayrhofer, P. H., Münz, W.-D., and Schenkel, M. (2008). Structure and mechanical properties of CrN/TiN multilayer coatings prepared by a combined HIPIMS/UBMS deposition technique. *Thin Solid Films, 517*(3), 1239-1244.
18. Paulitsch, J., Schenkel, M., Zufraß, T., Mayrhofer, P. H., and Münz, W.-D. (2010). Structure and properties of high power impulse magnetron sputtering and DC magnetron sputtering CrN and TiN films deposited in an industrial scale unit. *Thin Solid Films, 518*(19), 5558-5564.
19. Pelleg, J., Zevin, L., Lungo, S., and Croitoru, N. (1991). Reactive-sputter-deposited TiN films on glass substrates. *Thin Solid Films, 197*(1-2), 117-128.
20. Schönjahn, C., Donohue, L., Lewis, D., Münz, W.-D., Twesten, R., and Petrov, I. (2000). Enhanced adhesion through local epitaxy of transition-metal nitride coatings on ferritic steel promoted by metal ion etching in a combined cathodic arc/unbalanced magnetron deposition system. *Journal of Vacuum Science* and *Technology A: Vacuum, Surfaces,* and *Films, 18*(4), 1718-1723.
21. Takano, I., Isobe, S., Sasaki, T., and Baba, Y. (1989). Preparation of TiN thin films by the dynamic mixing method using an N2+ ion beam of 1 keV. *Thin Solid Films, 171*(2), 263-270.
22. Vasu, K., Krishna, M. G., and Padmanabhan, K. (2011). Substrate-temperature dependent structure and composition variations in RF magnetron sputtered titanium nitride thin films. *Applied Surface Science, 257*(7), 3069-3074.
23. Veiga, C., Davim, J., and Loureiro, A. (2012). Properties and applications of titanium alloys: a brief review. *Rev. Adv. Mater. Sci, 32*(2), 133-148.
24. Wang, F., Wu, M., Wang, Y., Yu, Y., Wu, X., and Zhuge, L. (2013). Influence of thickness and annealing temperature on the electrical, optical and structural properties of AZO thin films. *Vacuum, 89*, 127-131.
25. Xu, S., Du, L., Sugioka, K., Toyoda, K., and Jyumonji, M. (1998). Preferred growth of epitaxial TiN thin film on silicon substrate by pulsed laser deposition. *Journal of materials science, 33*(7), 1777-1782.
26. Zhao, J., Wang, X., Chen, Z. Y., Yang, S., Shi, T., and Liu, X. (1997). Overall energy model for preferred growth of TiN films during filtered arc deposition. *Journal of Physics D: Applied Physics, 30*(1), 5.

Downloaded from www.periodico.tchequimica.com

Figure 1. The main experimental set-up used in this work.

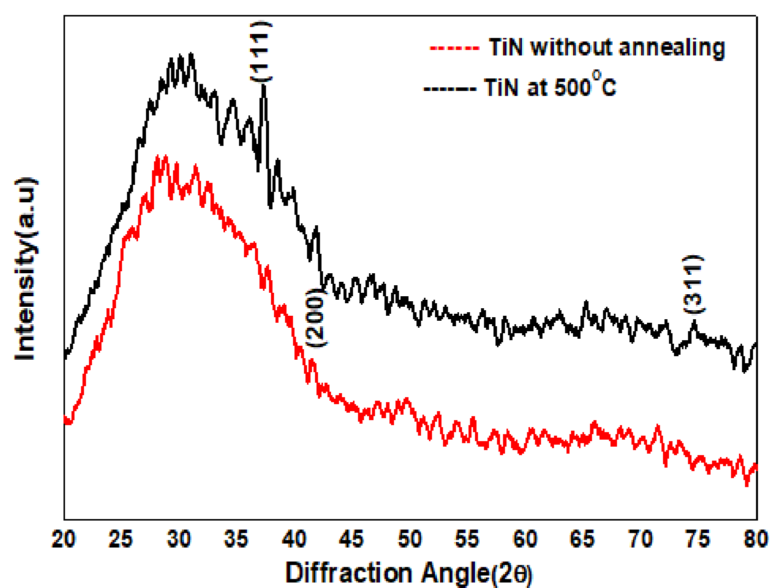

Figure 2. The X-ray diffraction of TiN films deposited on a glass substrate.

Downloaded from www.periodico.tchequimica.com

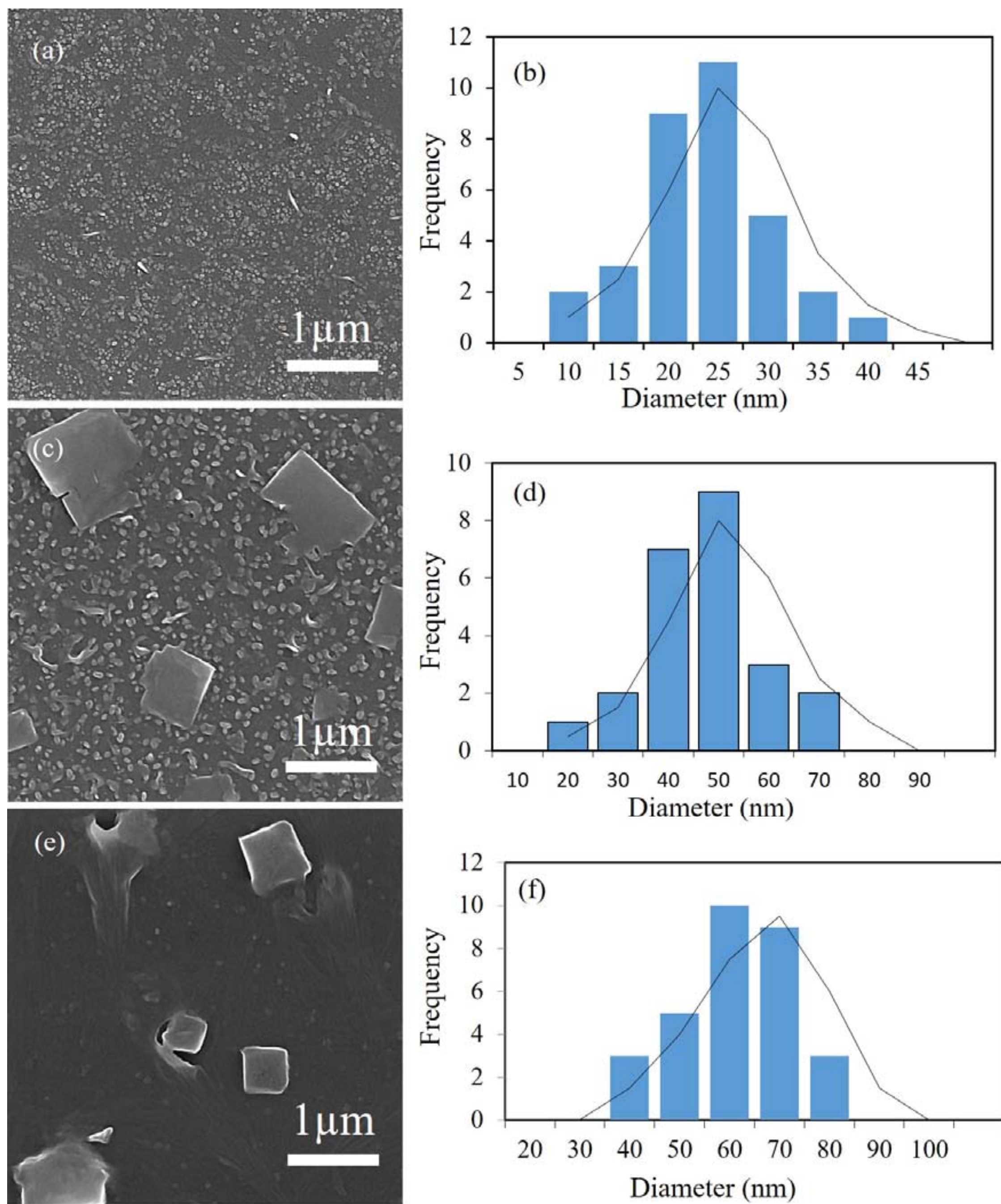

Figure 3. (a-b) FESEM image and histogram of TiN film before annealing, (c-d) FESEM image and histogram of TiN film coated at 400 °C, (e-f) FESEM image and histogram of TiN film coated at 500°C. TiN films deposited on glass substrates by D.C sputtering method.

Downloaded from www.periodico.tchequimica.com

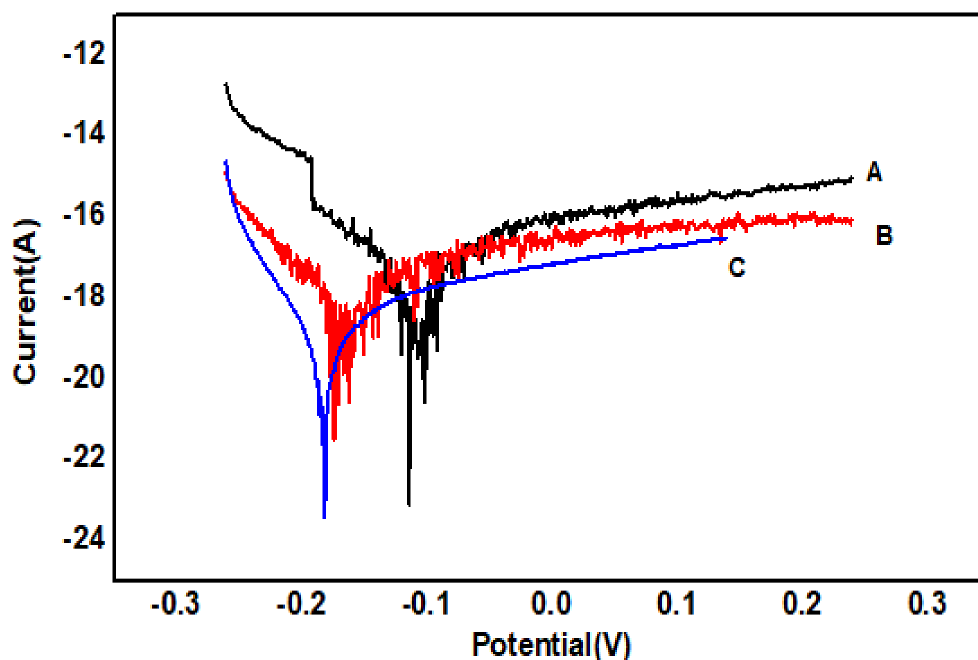

Figure 4. Polarization curves (Tafel) for TiN films deposited on Ti-6Al-4V alloy by D.C sputtering at 40 W for 2 hours. (A)Ti-6Al-4V alloy, (B) TiN coated Ti-6Al-4V alloy (C)TiN coated Ti-6Al-4V alloy with thermal annealing.

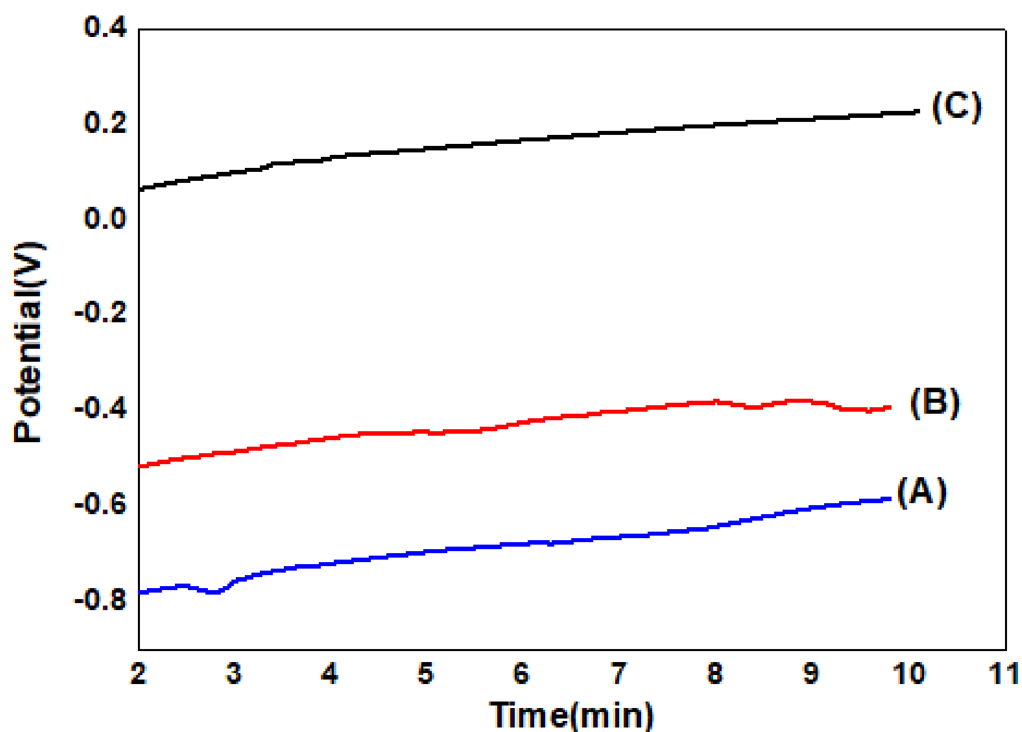

Figure 5. Open-circuit potential variation with time curve of TiN coated on Ti-6Al-4V alloy by D.C sputtering 40 W for 2 hours. (A)Ti-6Al-4V alloy, (B) TiN coated Ti-6Al-4V alloy (C) TiN coated Ti-6Al-4V alloy with thermal annealing.

Downloaded from www.periodico.tchequimica.com

***Table 1**. Reactive DC sputtering conditions for depositing TiN thin films*

Parameters	Values
Total pressure (Torr)	$5 \cdot 10^{-3}$
Sputtering power (Watt)	40
The target to substrate distance (mm)	60
Substrates	glass, Ti6AL4V
Gases mixture ratio ($Ar:N_2$)	(90:10)
Deposition time (hour)	2
Substrate temperature	373K

***Table 2**. Corrosion characteristics of Ti-6Al-4V samples coated with TiN.*

Item	$I_{corr.}$ Amp/cm^2	β_a (vol)	β_c (vol)	Corrosion potential (vol)	Corr.Rate (mm/y)	Rp KΩ/cm^2	Weight loss (mg.cm^{-2}.s^{-1})
Ti6Al4V alloy	$2.528 \cdot 10^{-7}$	0.097	0.587	-0.117	0.145	1.719	$2.043 \cdot 10^{-9}$
TiN coated Ti-6Al-4V alloy	$4.632 \cdot 10^{-8}$	0.069	0.569	-0.054	$2.667 \cdot 10^{-3}$	580	$3.738 \cdot 10^{-11}$
TiN coated Ti-6Al-4V alloy with thermal annealing.	$4.654 \cdot 10^{-9}$	0.049	0.119	-0.048	$2.685 \cdot 10^{-4}$	3247	$3.763 \cdot 10^{-12}$

Downloaded from www.periodico.tchequimica.com

The Periódico Tchê Química (ISSN: 1806-0374; 2179-0302) is an open-access journal since 2004. Journal DOI: 10.52571/PTQ. http://www.tchequimica.com.
This text was introduced in this file in 2021 for compliance reasons.
© The Author(s) OPEN ACCESS.
This article is licensed under a Creative Commons Attribution 4.0 (CC BY 4.0) International License, which permits use, sharing, adaptation, distribution, and reproduction in any medium or format, as long as you give appropriate credit to the original author(s) and the source, provide a link to the Creative Commons license, and indicate if changes were made. The images or other third-party material in this article are included in the article 's Creative Commons license unless indicated otherwise in a credit line to the material . If material is not included in the article's Creative Commons license and your intended use is not permitted by statutory regulation or exceeds the permitted use, you will need to obtain permission directly from the copyright holder. To view a copy of this license, visit http://creativecommons.org/licenses/by/4.0/.